Enhanced humanization and affinity maturation of neutralizing anti-hepatitis B virus preS1 antibody based on antigen–antibody complex structure

Jin Hong Kim[1], Philippe Gripon[2], Fidaa Bouezzedine[2], Mun Sik Jeong[1,3], Seung-Wook Chi[4], Seong-Eon Ryu[5], and Hyo Jeong Hong[1,3*]

[1]Institute of Antibody Research, Kangwon National University, Chuncheon 200-701, Korea

[2]Institut de Recherche Santé Environnement et Travail (IRSET) - U.1085, Institut National de la Santé et de la Recherche Médicale (Inserm), Rennes, Bretagne, France ; Université de Rennes 1, Rennes, Bretagne, France ; Structure Fédérative Biosit UMS 3480 CNRS-US18 Inserm, Rennes, Bretagne, France

[3]Department of Systems Immunology, College of Biomedical Science, Kangwon National University, Chuncheon 200-701, Korea

[4]Medical Proteomics Research Center, Korea Research Institute of Bioscience and Biotechnology, Daejeon 305-806, Korea

[5]Department of Bio-engineering and Institute for Bioengineering and Biopharmaceutical Research, Hanyang University, Seoul 133-791, Korea

[*]Corresponding author: e-mail address: hjhong@kangwon.ac.kr, phone +82-33-250-8381, fax +82-33-259-5643

Abstract

To improve a previously constructed broadly neutralizing hepatitis B virus (HBV)-specific preS1 humanized antibody (HzKR127), we further humanized it through specificity-determining residue (SDR) grafting. Moreover, we improved affinity by mutating two residues in heavy-chain complementarity-determining regions (CDR), on the basis of the crystal structure of the antigen–antibody complex. HzKR127-3.2 exhibited 2.5-fold higher affinity and enhanced virus-neutralizing activity compared to the original KR127 antibody and showed less immunogenic potential than HzKR127. Enhanced virus-neutralizing activity was achieved by the increased association rate, providing insights into engineering potent antibody therapeutics for HBV immunoprophylaxis. HzKR127-3.2 may be a good candidate for HBV immunoprophylaxis.

Keywords: humanized antibody; specificity-determining residue grafting; affinity maturation; HBV; preS1; virus neutralization

1. Introduction

Over the last three decades, monoclonal antibodies (mAbs) have emerged as powerful human therapeutics due to advances in antibody engineering technologies [1]. Nonhuman antibodies induce an immune response in humans, which limits their therapeutic use [2]. To overcome this problem, humanized antibodies have been constructed by grafting the complementarity-determining regions (CDRs) of murine mAbs onto human framework regions (FRs), which is commonly referred to as CDR grafting [3]. Simple grafting of CDRs, however, often decreases affinity, because some FR residues directly contact the antigen or support conformation of the CDR loops [4, 5]. Therefore, humanized antibodies are usually constructed by CDR grafting while retaining those mouse FR residues that influence antigen-binding activity [6, 7]. These humanized antibodies are generally less immunogenic in patients than chimeric antibodies that are composed of mouse variable domains and human constant domains; however, they may still be immunogenic since the CDRs are not human [8, 9]. Therefore, to minimize the immunogenicity of humanized antibodies, only the mouse CDR residues that influence antigen binding (i.e., specificity-determining residues, or SDRs) are retained, while those that are not involved in antigen binding are replaced by human counterparts [10-13]. SDR-grafted humanized antibodies exhibit less immunogenic potential than CDR-grafted humanized antibodies.

HBV is a worldwide public health problem that affects 240 million chronic carriers, who have a high risk of developing hepatocellular carcinoma [14]. The HBV envelope contains three related surface glycoproteins called the large (L), middle (M), and small (S) proteins. These proteins are the product of a single open reading frame that is divided into preS1, preS2, and S regions [15]. The S protein is encoded by the S region; the M protein contains the preS2 and S antigens; and the L protein contains the preS1, preS2, and S antigens. The three antigens have been shown to elicit virus-neutralizing antibodies [16-20]. In particular, the preS1(amino acids 2–48, *ayw* subtype) of the L protein and the common “a” determinant of the S antigen have been shown to play an essential role in viral infectivity [21-27]. Recently a cellular receptor for the pre-S1 sequence was identified as sodium taurocholate transporter (NTCP) [28], while heparin sulfate proteoglycan (HSPG) was recognized as a binding partner for the “a” determinant [29]. For immunoprophylaxis of HBV infection, hepatitis B immune globulin (HBIG) prepared from pooled human anti-HBsAg plasma is administered to infants born of HBsAg-HBeAg–positive mothers, to susceptible individuals with acute exposure to infectious HBV-containing material, and to orthotopic liver transplant

patients with chronic HBV-related liver disease [30-32]. However, the currently available HBIG is not an ideal source of antibody due to its limited availability and low specific activity. Virus-neutralizing mAbs against the preS1 and S antigens would be an effective alternative for immunoprophylaxis of HBV infection.

We previously generated a murine mAb (KR127) that recognizes amino acids 37–45 (NSNNPDWDF) of the preS1 of *adr* subtype, corresponding to aa 26–34 of *ayw* subtype, and subsequently constructed a humanized antibody (HzKR127) by CDR grafting. HzKR127 retained the same epitope specificity and affinity as KR127 and exhibited HBV-neutralizing activity in chimpanzees [33-35]. In addition, we determined the crystal structure of the HzKR127 antigen-binding fragment (Fab) and its complex with the epitope to understand the structural mechanisms of the antigen–antibody interaction [36].

In the present study, based on the structural information, we further humanized HzKR127 by SDR grafting and also improved its affinity by mutating two heavy-chain CDR residues. The resulting humanized antibody (HzKR127-3.2) exhibited higher HBV-neutralizing activity than KR127 and lower immunogenic potential than HzKR127. The enhanced virus-neutralizing activity was achieved by an increase in the association rate. This information will be useful for the design and development of potent antibody therapeutics against HBV, and this advanced humanized antibody may be a good candidate for immunoprophylaxis of HBV infection.

2. Materials and methods

2.1. Cell culture

HEK293T, ACHN, B16F1, and SCK-L1 [37] cells were grown in DMEM (Invitrogen) supplemented with 10% FBS. CHO-DG44 cells were grown in DMEM/F12 (Invitrogen) with supplements as described previously [35]. HepaRG cells were cultured and differentiated as previously described [24] and maintained after seeding into 96-well plates in William's E medium (Gibco Life technologies) supplemented with 5% fetal calf serum, 2% DMSO, 5 mg/L insulin, 5×10^{-6} M hydrocortisone, 5 µg/L sodium selenite, 20,000 UI/L penicillin, and 20 mg/L streptomycin. All cells were cultured in 5% CO_2 in a 37°C humidified incubator.

2.2. Construction, expression, and purification of humanized antibodies

Humanized VH and VL genes were synthesized by GeneArt (Germany) and sequentially subcloned into the EcoRI-ApaI and HindIII-BsiWI sites, respectively, of pdCMV-dhfrC-

cA10A3 containing human Cγ1 and Cκ. The resulting expression plasmids were introduced into HEK293T cells using Lipofectamine (Invitrogen). The culture supernatant was subjected to affinity chromatography on a protein A–sepharose column (Millipore), and the protein concentration was determined with a NanoDrop (Thermo Scientific) based on the molar extinction coefficient. The integrity of the purified protein was analyzed by SDS-PAGE.

2.3. Affinity determination

Competition ELISA was performed as described previously [38]. Briefly, a solution containing 5–10 ng of each antibody and various concentrations (10^{-10}–10^{-6} M) of GST-preS1 (amino acids 1–56) as a competing antigen were preincubated at 37°C for 3 h. The mixtures were then added to each well, which had been coated with 100 ng of GST-preS1. Bound antibody was detected by indirect ELISA.

For affinity determination by Octet Red, anti-human Fc–coated biosensor tips (ForteBio, 18-0015) were activated in PBS with 0.1% w/v bovine serum albumin (0.1% PBA) for 20 min by agitating 96-well microtiter plates (Greiner bio-one, 655209) at 1000 rpm and then saturated with 2 μg/mL antibody for 10 min. This typically resulted in capture levels of 1 nm. GST-preS1 was prepared as a 2-fold serial dilution (6.25, 12.5, 25, 50, and 100 nM) in 0.1% PBA and separately incubated with the antibody bound on the tips. Association and dissociation rates were measured for 15 and 30 min, respectively. All measurements were corrected for baseline drift by subtracting a control sensor exposed to running buffer only. Operating temperature was maintained at 30°C. Data were analyzed using a 1:1 interaction model (fitting global, Rmax unlinked by sensor) with ForteBio data analysis software 7.0.

2.4. Western blot analysis

GST-preS1 (amino acids 1–56) and each of the alanine replacement mutants of the preS1 (amino acids 37–47) were expressed in *E. coli* DH5α cells as described previously [38]. Protein extracts were subjected to 12% SDS-PAGE and western blot analysis with KR127 or humanized KR127 antibody (1 μg/ml), followed by anti-mouse or human IgG (Fc-specific)–HRP conjugate (1:5000 v/v, Thermo Scientific).

2.5. Flow cytometric analysis

Cells were incubated with 1 μg of antibody in 100 μl of PBA for 60 min at 4°C. After washing three times with PBA, the cells were incubated with a fluorescein isothiocyanate–

conjugated anti-hFc antibody (BD Pharmingen) for 30 min at 4°C. Propidium iodide–negative cells were analyzed for antibody binding using FACSCalibur (Becton Dickinson).

2.6. *In vitro* HBV infection and neutralization assays

In vitro HBV infection and neutralization assays were carried out using differentiated HepaRG cells and *adr* or *ayw* subtype of HBV particles. The *ayw* viral particles were produced by transient transfection of HepG2 cells [39] with plasmid (pHBVEcoR1-) containing an overlength HBV genome originally described in Gripon et al. [40], and supernatants from the transfected cells were concentrated fifty-fold by PEG precipitation as previously described [23]. The genomic sequence of the *ayw* subtype corresponds to the sequence (genebank accession number V01460.1) published by Galibert et al. [41], corresponding to genotype D by online genotyping analysis [42]. The *adr* particles were produced and concentrated by the same procedures using the pHBV 5.2 [43] containing the preS1 sequence [44] that was identified as genotype C by the online genotyping analysis.

For *in vitro* HBV infection, HepaRG cells were seeded at a density of 6×10^4 cells per well (containing 100 µl of culture medium) and were infected 6 days later with the *adr* or *ayw* viral particles (about 6×10^6 viral genomic equivalent). HBV infection was also performed in the presence of 4% PEG 8000 and a five-fold diluted inoculum. PEG was added during the infection process, which allows a great enhancement of viral infectivity without compromising the specificity of the infection process as previously described [45]. To evaluate binding of antibody to the viral particles present in the HBV inocula, ELISA plates were coated with either KR127 or HzKR127-3.2 (1 µg/ml) in a carbonate buffer overnight at room temperature. After saturation with 5% fetal calf serum for 2 h at room temperature, serially diluted HBV inocula were added and incubated for 4 h at room temperature. The bound viral particles were then detected with an anti-HBs antibody conjugated with peroxidase from a HBs detection kit (Bio-Rad).

For the neutralization assay, the *adr* or *ayw* viral particles (5 µl) were preincubated with 5 µl of antibody at the indicated concentrations at room temperature for 30 min and then incubated with cultured HepaRG cells covered with 100 µl of the culture medium for 24 hours in the absence or presence of 4% PEG 8000. The infected cells were washed with the medium and further incubated for 10 days, with the medium changed every 2 days. On day 10 postinfection, the culture supernatant was diluted in order to remain in the quantitative

range of the assay and the HBsAg concentration was determined with an ELISA kit (Bio-Rad).

3. Results

3.1. Construction of humanized antibody HzKR127-3 by SDR grafting

We previously constructed an anti-preS1 humanized antibody (HzKR127) from the murine mAb KR127 by CDR grafting. In HzKR127, the CDRs of mouse VH and VL were grafted into human germline segments DP7-JH4 and DPK12-JK4, respectively, while eleven FR residues in the mouse VH and five FR residues in the mouse VL that were thought to influence the CDR loops or to stabilize the structure of the variable regions were retained [35]. The amino acid sequences of the VH and VL of KR127 and HzKR127 are shown in Figure 1. In this study, we further humanized HzKR127 by SDR grafting and increased its affinity by site-directed mutagenesis.

For SDR grafting, mouse residues that are buried and/or not involved in antigen binding are replaced by human counterparts, based on the previously determined three-dimensional structure of the antigen–antibody complex [36].For the VH, nine mouse FR residues (Val12, Ala28, Ser30, Ile48, Lys66, Ala67, Leu69, Ala78, and Phe91) were replaced by human residues, while two mouse FR3 residues (Ala71 and Lys73) that are involved in the interaction with HCDR2 loop were retained. Ala71 is in hydrophobic interaction with Ile51 and Pro53, and Lys 73 is in hydrogen bonding with Gly54 (Fig. 2A). For the VL, three mouse FR residues (Leu3, Ser43, and Lys45) were replaced by human residues, while two mouse FR2 residues (Leu36 and Arg46) were retained. Leu36 forms a tight interaction with Trp103 of VH in the bottom of the antigen-binding pocket and is close to the Glu98 side chain of the HCDR3 loop (Fig. 2B). Thus, mutation of Leu36 to Tyr is likely to disturb the conformation of the antigen-binding pocket and prohibit optimal binding to the antigen. Residue Arg46 forms a salt bridge with Asp97 in HCDR3, which stabilizes the conformation of HCDR3 in the free structure (Fig. 3A). In addition to the FR residues, two LCDR2 residues (Lys53 and Leu54) were replaced by human residues because they are not involved in antigen binding (Fig. 2C).

The designed humanized VH and VL sequences were synthesized and combined with human Cγ1 and Cκ, respectively, to construct expression plasmid pdCMV-dhfrC-HzKR127-3. This plasmid DNA was introduced into HEK293T cells, and the resulting humanized antibody (HzKR127-3) was purified from the culture supernatant. Affinity determination by

competition ELISA indicated that the affinity of HzKR127-3 for GST-preS1 was slightly lower than that of the original KR127 antibody (Supplemental Fig. S1). Affinity determination by Octet Red indicated that HzKR127-3 had approximately 3-fold lower affinity (K_D) compared to KR127; this decrease was due mostly to an increase in the dissociation rate (Supplemental Fig. S2A and S2B and Table 1).

3.2. Affinity maturation of HzKR127-3

In our previous structural study, a comparison of the structures of free HzKR127 Fab and its complex with the preS1 epitope revealed that the HCDR3 loop undergoes the most noticeable conformational change between the free and complex structures, illustrating a lid-opening mechanism for antigen binding [36]. As shown in Figure 3A, the Asp97 residue is not involved in a direct interaction with the preS1 antigen; rather, it forms a salt bridge with Arg46 in the light chain FR2, which stabilizes closing of the HCDR3 lid in the free structure. However, upon antigen binding, the HCDR3 loop lid is opened and an antigen-binding pocket is thereby created, leading to tight locking in of the peptide (Fig. 3B). Residue Asp97 is located at the apex of the HCDR3 lid and undergoes the largest movement, with a 9.6 Å shift in the main chain upon lid opening (Supplemental Fig. S3). Alanine mutation of the Asp97 would disrupt the salt bridge, making the HCDR3 loop more flexible. This could facilitate the structural transition from the closed to the open state, thus leading to an increase in affinity. We therefore substituted an alanine for Asp97 of HzKR127-3. The resulting antibody (HzKR127-3.1) was transiently expressed in HEK293T cells, purified, and subjected to affinity determination by competition ELISA followed by Octet Red. The affinity of HzKR127-3.1 (8.13×10^{-10} M) was 4.9-fold higher than that of HzKR127-3 (3.97×10^{-9} M), and the increase in affinity was achieved mostly by a decrease in the dissociation rate (Supplemental Fig. S1 and S2C and Table 1).

In an attempt to further increase the affinity of HzKR127-3.1, Asn58 in HCDR2 of HzKR127-3.1 was mutated to alanine and subjected to competition ELISA, which showed an increase in affinity (data not shown). This indicates that Asn58 is not optimal for antigen binding. We speculated that the replacement of Asn58 by alanine, which has a smaller side chain, would give the preS1 epitope easier access to the antigen-binding pocket, which could result in a faster association rate (Fig. 2D). Therefore, Asn58 was replaced by the human counterpart (Ser58) as a first choice. The resulting humanized antibody (HzKR127-3.2) was transiently expressed, purified, and subjected to affinity determination. The affinity of

HzKR127-3.2 (4.93×10^{-10} M) was 1.6-fold higher than that of HzKR127-3.1, and the increased affinity was achieved mostly by an increase in the association rate (Supplemental Fig. S1 and S2D and Table 1).

3.3. Analysis of potential immunogenicity of HzKR127-3.2

The VH and VL sequences of HzKR127 and HzKR127-3.2 were analyzed with ProPred [46] to identify potential T cell epitopes that bind to MHC II molecules (HLA-DR). This is based on the fact that the peptide–MHC II complexes are recognized by helper T cells and trigger the activation and differentiation of helper T cells to stimulate the immune response. As summarized in Table 2, potential T cell epitopes detected at the junction between HCDR2 and FR3 (HCDR2/FR3) or in the light chain FR2 of HzKR127 were eliminated in HzKR127-3.2, while those detected at the junction between light chain FR2 and LCDR2 (FR2/LCDR2) were greatly reduced.

3.4. Specificity of HzKR127-3.2

To confirm the antigen-binding specificity of HzKR127-3.2, a series of GST-preS1 (amino acids 1–56) proteins that individually carry an alanine replacement mutation at each position in the preS1 epitope were expressed in *E. coli* and subjected to western blot analysis with KR127 or HzKR127-3.2. As shown in Figure 4A, HzKR127-3.2 exhibited the same epitope specificity as that of KR127.

In addition, to determine whether HzKR127-3.2 does not exhibit off-target activity, flow cytometric analysis was performed. To prepare preS1-expressing cells (293T-S1-L1) as a positive control, preS1 (amino acids 37–47) was fused to the N-terminus of the integral membrane protein L1 cell adhesion molecule (L1CAM). The fusion protein was then transiently expressed in HEK293T cells. HzKR127-3.2 bound to the surface of the 293T-S1-L1 cells but did not bind to preS1-negative cells such as HEK293T, L1CAM-overexpressing human cholangiocarcinoma (SCK-L1), human renal carcinoma (ACHN), mouse melanoma (B16F1), and Chinese hamster ovary (CHO) cells (Fig. 4B).

3.5. Evaluation of HBV-neutralizing activity of HzKR127-3.2

Because HzKR127-3.2 exhibited higher affinity for the preS1 antigen than KR127, we compared their virus-neutralizing activities by *in vitro* HBV-neutralization assay. To begin with, we confirmed binding of the antibodies to the viral particles. As shown in Figure 5A,

the antibodies bound to the *ayw* and *adr* particles in a dose-dependent manner, and HzKR127-3.2 bound more efficiently compared to KR127. Next, HepaRG cells were infected with either the *adr* or *ayw* subtype of HBV particles, which had been preincubated with different concentrations (0.2–200 μg/ml) of each antibody. The infected cells were then cultured for 10 days, and the growth medium was changed every 2 days. On day 10 postinfection, HBsAg secretion by the infected cells was measured by ELISA. As shown in Figure 5B and 5C, the HBsAg secretion rate gradually decreased with increasing antibody concentration, demonstrating the specificity of the neutralization assay, and HzKR127-3.2 exhibited enhanced virus-neutralizing activity against both *adr* and *ayw* subtypes compared to KR127.

We also performed the HBV infection and neutralization assay in the presence of 4% PEG 8000. The presence of PEG increases the infectivity and thus allowed to use five-fold diluted inoculum without compromising infectivity [45]. Because this assay has a higher ratio of antibody molecules to viral particles compared to the assay in the absence of PEG, it was expected to improve the neutralization activity of the antibodies, although it is not under physiological conditions. Indeed the infection level was higher since HBsAg production reached 100 ng/ml, and an almost complete neutralization was observed with the highest antibody dose, while HzKR127-3.2 neutralized the viral particles more efficiently than KR127 (Supplemental Fig. S4).

4. Discussion

We had previously constructed the CDR-grafted humanized antibody HzKR127; the epitope specificity and affinity of HzKR127 are the same as those of the original murine mAb, KR127. HzKR127 virus-neutralizing activity was confirmed in chimpanzees. Subsequently, the crystal structures of HzKR127 Fab and its complex with the epitope revealed that HzKR127 exerts a lid-opening mechanism for antigen binding, one of the largest conformational changes in antigen–antibody recognition. In the present study, we successfully optimized HzKR127 through SDR grafting and affinity maturation by rational design based on the antigen–antibody complex structure. A total of 15 (12 in FR, one in HCDR2, and two in LCDR2) mouse residues in HzKR127 were replaced by human residues, and Asp97 in HCDR3 was replaced by alanine. The resulting humanized antibody (HzKR127-3.2) exhibited 2.5-fold higher affinity for the preS1 antigen and enhanced virus-neutralizing activity against both *adr* and *ayw* subtypes of HBV compared to KR127.

Moreover, it retained the same epitope specificity as that of KR127 and did not show any off-target activity, as assessed by flow cytometric analysis. In addition, T epitope analysis suggested that HzKR127-3.2 may be less immunogenic in humans than HzKR127. Considering that HzKR127 exhibited virus-neutralizing activity in chimpanzees, HzKR127-3.2 might exhibit higher *in vivo* virus-neutralizing activity than HzKR127 and thus may be more effective in the immunoprophylaxis of HBV infection. HzKR127-3.2 may be particularly useful for repeated administration to humans because of its minimized immunogenic potential.

KR127 and HzKR127-3.2 target amino acids 37-45 from the L protein of *adr* subtype, corresponding to amino acids 26-34 of *ayw* subtype. This epitope lies in preS1 region of the L protein which is involved in HBV infectivity, since the target of the peptide(amino acids 2-47, *ayw* subtype) was identified as NTCP and shown to be a functional receptor for HBV entry [28]. Therefore, our antibodies target a region crucial for HBV infectivity and thus were expected to block entry. However, Bremer *et al*. reported that antibodies against preS1(1-21) of *ayw* subtypes reacted well with non-myristoylated preS1 peptides but only weakly with myristoylated preS1 peptides and did not neutralize the infectivity of HBV, whereas antibodies to neighboring sequences neutralized very well [47]. The data suggest that antibodies to preS1(22-47) of *ayw* subtypes are likely to bind well to HBV and neutralize viral infectivity. Indeed, we observed that HzKR127-3.2 recognizing preS1(37-45) of *adr* subtypes bound to the viral particles of both *ayw* and *adr* subtypes and neutralized them efficiently. Analysis of antigen-antibody interaction of HzKR127-3.2 indicated that seven residues in the epitope sequence, except Ser38 and Asn39, are essential for antibody binding (Figure 4). Among the essential residues, five residues (Asn37, Pro41, Asp42, Trp43, and Asp44) are highly conserved among genotypes [28], while the other two residues (Asn40 and Phe45) are infrequently changed to serine and leucine or histidine, respectively in some genotypes. Neutralization efficiency of HzKR127-3.2 against these genotypes remains to be determined.

Regarding the correlation between kinetic parameters and virus-neutralizing potency, studies with mAbs against respiratory syncytial virus (RSV) F protein have shown that a direct relationship exists between the association rate and RSV-neutralizing activity [48-50], while studies with other viral pathogens, such as human immunodeficiency virus or rotavirus, have shown that virus-neutralizing activity can be determined predominantly by the dissociation rate [51, 52]. In case of HBV-neutralizing antibody, a recent study showed no

correlation between the affinity of anti-S monoclonal antibodies and their ability to neutralize HBV infection [53]. In this study, HzKR127-3.2 exhibited 2.5-fold higher affinity for the preS1 and enhanced *in vitro* virus-neutralizing activity against both *adr* and *ayw* subtypes of HBV compared to KR127, while the association rate was 2.3-fold faster and the dissociation rate was slightly slower. These data indicate that the enhanced virus-neutralizing activity was achieved by an increased association rate, which suggests that the association rate of anti-preS1 antibodies may play a predominant role in HBV neutralization. To the best of our knowledge, this is the first study to show a direct relationship between the association rate and neutralizing potency in antibody-mediated HBV neutralization. Our findings may provide insights that will help to facilitate the engineering of potent antibody therapeutics for HBV immunoprophylaxis.

Acknowledgments

This work was supported by Ministry of Health and Welfare grant A050260 and by a 2014 research grant from Kangwon National University (No. 120140400). This work was also financially supported by ANRS (Agence nationale de recherche contre le sida et les hépatites virales). Fidaa Bouezzedine was recipient of a fellowship from the Ligue Nationale Contre le Cancer. Manipulations of pathogens were performed in the biosafety level 3 containment laboratory core facility of the Biology and Health Federative Research Structure of Rennes (Biosit).

References

1. Buss, N.A., et al., *Monoclonal antibody therapeutics: history and future.* Curr Opin Pharmacol, 2012. **12**(5): p. 615-22.
2. Shawler, D.L., et al., *Human immune response to multiple injections of murine monoclonal IgG.* J Immunol, 1985. **135**(2): p. 1530-5.
3. Jones, P.T., et al., *Replacing the complementarity-determining regions in a human antibody with those from a mouse.* Nature, 1986. **321**(6069): p. 522-5.
4. Queen, C., et al., *A humanized antibody that binds to the interleukin 2 receptor.* Proc Natl Acad Sci U S A, 1989. **86**(24): p. 10029-33.
5. Al-Lazikani, B., A.M. Lesk, and C. Chothia, *Standard conformations for the canonical structures of immunoglobulins.* J Mol Biol, 1997. **273**(4): p. 927-48.
6. Winter, G. and W.J. Harris, *Humanized antibodies.* Immunol Today, 1993. **14**(6): p. 243-6.
7. Safdari, Y., et al., *Antibody humanization methods - a review and update.* Biotechnol Genet Eng Rev, 2013. **29**(1-2): p. 175-86.
8. Hwang, W.Y. and J. Foote, *Immunogenicity of engineered antibodies.* Methods, 2005. **36**(1): p. 3-10.

9. Harding, F.A., et al., *The immunogenicity of humanized and fully human antibodies: residual immunogenicity resides in the CDR regions.* MAbs, 2010. **2**(3): p. 256-65.
10. Padlan, E.A., *Anatomy of the antibody molecule.* Mol Immunol, 1994. **31**(3): p. 169-217.
11. Gonzales, N.R., et al., *SDR grafting of a murine antibody using multiple human germline templates to minimize its immunogenicity.* Mol Immunol, 2004. **41**(9): p. 863-72.
12. Yoon, S.O., et al., *Construction, affinity maturation, and biological characterization of an anti-tumor-associated glycoprotein-72 humanized antibody.* J Biol Chem, 2006. **281**(11): p. 6985-92.
13. Kim, K.S., et al., *Construction of a humanized antibody to hepatitis B surface antigen by specificity-determining residues (SDR)-grafting and de-immunization.* Biochem Biophys Res Commun, 2010. **396**(2): p. 231-7.
14. Ganem, D. and A.M. Prince, *Hepatitis B virus infection--natural history and clinical consequences.* N Engl J Med, 2004. **350**(11): p. 1118-29.
15. Heermann, K.H., et al., *Large surface proteins of hepatitis B virus containing the pre-s sequence.* J Virol, 1984. **52**(2): p. 396-402.
16. Dreesman, G.R., et al., *Antibody to hepatitis B surface antigen after a single inoculation of uncoupled synthetic HBsAg peptides.* Nature, 1982. **295**(5845): p. 158-60.
17. Heermann, K.H., et al., *Immunogenicity of the gene S and Pre-S domains in hepatitis B virions and HBsAg filaments.* Intervirology, 1987. **28**(1): p. 14-25.
18. Itoh, Y., et al., *A synthetic peptide vaccine involving the product of the pre-S(2) region of hepatitis B virus DNA: protective efficacy in chimpanzees.* Proc Natl Acad Sci U S A, 1986. **83**(23): p. 9174-8.
19. Klinkert, M.Q., et al., *Pre-S1 antigens and antibodies early in the course of acute hepatitis B virus infection.* J Virol, 1986. **58**(2): p. 522-5.
20. Neurath, A.R., B. Seto, and N. Strick, *Antibodies to synthetic peptides from the preS1 region of the hepatitis B virus (HBV) envelope (env) protein are virus-neutralizing and protective.* Vaccine, 1989. **7**(3): p. 234-6.
21. Neurath, A.R., et al., *Identification and chemical synthesis of a host cell receptor binding site on hepatitis B virus.* Cell, 1986. **46**(3): p. 429-36.
22. Pontisso, P., et al., *Identification of an attachment site for human liver plasma membranes on hepatitis B virus particles.* Virology, 1989. **173**(2): p. 522-30.
23. Le Seyec, J., et al., *Infection process of the hepatitis B virus depends on the presence of a defined sequence in the pre-S1 domain.* J Virol, 1999. **73**(3): p. 2052-7.
24. Gripon, P., et al., *Infection of a human hepatoma cell line by hepatitis B virus.* Proc Natl Acad Sci U S A, 2002. **99**(24): p. 15655-60.
25. Glebe, D., et al., *Pre-s1 antigen-dependent infection of Tupaia hepatocyte cultures with human hepatitis B virus.* J Virol, 2003. **77**(17): p. 9511-21.
26. Gripon, P., I. Cannie, and S. Urban, *Efficient inhibition of hepatitis B virus infection by acylated peptides derived from the large viral surface protein.* J Virol, 2005. **79**(3): p. 1613-22.
27. Salisse, J. and C. Sureau, *A function essential to viral entry underlies the hepatitis B virus "a" determinant.* J Virol, 2009. **83**(18): p. 9321-8.
28. Yan, H., et al., *Sodium taurocholate cotransporting polypeptide is a functional receptor for human hepatitis B and D virus.* Elife, 2012. **1**: p. e00049.
29. Sureau, C. and J. Salisse, *A conformational heparan sulfate binding site essential to infectivity overlaps with the conserved hepatitis B virus a-determinant.* Hepatology,

2013. **57**(3): p. 985-94.
30. Beasley, R.P., et al., *Prevention of perinatally transmitted hepatitis B virus infections with hepatitis B immune globulin and hepatitis B vaccine.* Lancet, 1983. **2**(8359): p. 1099-102.
31. McGory, R.W., et al., *Improved outcome of orthotopic liver transplantation for chronic hepatitis B cirrhosis with aggressive passive immunization.* Transplantation, 1996. **61**(9): p. 1358-64.
32. Terrault, N.A., et al., *Prophylaxis in liver transplant recipients using a fixed dosing schedule of hepatitis B immunoglobulin.* Hepatology, 1996. **24**(6): p. 1327-33.
33. Ryu, C.J., et al., *Mouse monoclonal antibodies to hepatitis B virus preS1 produced after immunization with recombinant preS1 peptide.* Hybridoma, 2000. **19**(2): p. 185-9.
34. Maeng, C.Y., et al., *Fine mapping of virus-neutralizing epitopes on hepatitis B virus PreS1.* Virology, 2000. **270**(1): p. 9-16.
35. Hong, H.J., et al., *In vivo neutralization of hepatitis B virus infection by an anti-preS1 humanized antibody in chimpanzees.* Virology, 2004. **318**(1): p. 134-41.
36. Chi, S.W., et al., *Broadly neutralizing anti-hepatitis B virus antibody reveals a complementarity determining region H3 lid-opening mechanism.* Proc Natl Acad Sci U S A, 2007. **104**(22): p. 9230-5.
37. Min, J.K., et al., *L1 cell adhesion molecule is a novel therapeutic target in intrahepatic cholangiocarcinoma.* Clin Cancer Res, 2010. **16**(14): p. 3571-80.
38. Oh, M.S., et al., *A new epitope tag from hepatitis B virus preS1 for immunodetection, localization and affinity purification of recombinant proteins.* J Immunol Methods, 2003. **283**(1-2): p. 77-89.
39. Sells, M.A., M.L. Chen, and G. Acs, *Production of hepatitis B virus particles in Hep G2 cells transfected with cloned hepatitis B virus DNA.* Proc Natl Acad Sci U S A, 1987. **84**(4): p. 1005-9.
40. Gripon, P., et al., *Myristylation of the hepatitis B virus large surface protein is essential for viral infectivity.* Virology, 1995. **213**(2): p. 292-9.
41. Galibert, F., et al., *Nucleotide sequence of the hepatitis B virus genome (subtype ayw) cloned in E. coli.* Nature, 1979. **281**(5733): p. 646-50.
42. Hayer, J., et al., *HBVdb: a knowledge database for Hepatitis B Virus.* Nucleic Acids Res, 2013. **41**(Database issue): p. D566-70.
43. Ryu, C.J., et al., *In vitro neutralization of hepatitis B virus by monoclonal antibodies against the viral surface antigen.* J Med Virol, 1997. **52**(2): p. 226-33.
44. Kim, H.S. and H.J. Hong, *Efficient expression, purification and characterization of hepatitis B virus preS1 from Escherichia coli.* Biotechnology letters, 1995. **17**(8): p. 871-6.
45. Gripon, P., C. Diot, and C. Guguen-Guillouzo, *Reproducible high level infection of cultured adult human hepatocytes by hepatitis B virus: effect of polyethylene glycol on adsorption and penetration.* Virology, 1993. **192**(2): p. 534-40.
46. Singh, H. and G.P. Raghava, *ProPred: prediction of HLA-DR binding sites.* Bioinformatics, 2001. **17**(12): p. 1236-7.
47. Bremer, C.M., et al., *N-terminal myristoylation-dependent masking of neutralizing epitopes in the preS1 attachment site of hepatitis B virus.* J Hepatol, 2011. **55**(1): p. 29-37.
48. Wu, H., et al., *Ultra-potent antibodies against respiratory syncytial virus: effects of binding kinetics and binding valence on viral neutralization.* J Mol Biol, 2005. **350**(1): p. 126-44.

49. Wu, H., et al., *Development of motavizumab, an ultra-potent antibody for the prevention of respiratory syncytial virus infection in the upper and lower respiratory tract.* J Mol Biol, 2007. **368**(3): p. 652-65.
50. Bates, J.T., et al., *Reversion of somatic mutations of the respiratory syncytial virus-specific human monoclonal antibody Fab19 reveal a direct relationship between association rate and neutralizing potency.* J Immunol, 2013. **190**(7): p. 3732-9.
51. VanCott, T.C., et al., *Dissociation rate of antibody-gp120 binding interactions is predictive of V3-mediated neutralization of HIV-1.* J Immunol, 1994. **153**(1): p. 449-59.
52. Kallewaard, N.L., et al., *Functional maturation of the human antibody response to rotavirus.* J Immunol, 2008. **180**(6): p. 3980-9.
53. Shirazi., F.G., et al., *Monoclonal antibodies to various epitopes of hepatitis B surface antigen inhibit hepatitis B virus infection.* J Gastroenterol Hepatol, 2014. **29**(5): p. 1083-91.

Figure legends

Fig. 1. Amino acid sequences of VH (A) and VL (B) of murine antibody KR127 and humanized antibodies (HzKR127, HzKR127-3, HzKR127-3.1 and HzKR127-3.2). DP7 and DPK12 are the human Ig VH and Vκ germ-line segments, respectively. The dashes indicate identical amino acid residues.

Fig. 2. Crystal structure of the HzKR127 Fab–preS1 complex. (A) Interaction between the VH FR3 residue (Ala71H or Lys73H) and HCDR2 (H2) loop. (B) Interaction between the VL FR2 residue (Leu36L) and Trp103H in FR4. (C) Location of the LCDR2 residues (Leu54L and Lys53L). (D) Location of Asn58H in HCDR2. The VH and VL are shown in blue and in pink, respectively. The CDR loops and preS1 peptide are colored yellow and green, respectively.

Fig. 3. Hydrogen bonds between the HCDR3 lid (yellow) and neighboring residues in the free (A) and preS1-bound (B) HzKR127 Fab. The residues involved in the hydrogen bonds are labeled, and the hydrogen bonds are indicated as dotted lines. The preS1 peptide is shown in green. The light and heavy chains are colored pink and blue, respectively.

Fig. 4. Validation of epitope specificity (A) and off-target activity (B) of HzKR127-3.2. (A) GST-preS1 (amino acids 1–56) protein (WT) and a series of alanine replacement mutants were expressed in *E. coli* and subjected to 12% SDS-PAGE (bottom) followed by western blot analysis with KR127, HzKR127-3.1, or HzKR127-3.2 (Top). The protein band corresponding to the GST-preS1 is marked. (B) HzKR127-3.2 was subjected to flow cytometric analysis using preS1-expressing HEK293T cells (293T-S1-L1) and preS1-negative cells (HEK293T, SCK-L1, ACHN, B16F1, and CHO).

Fig. 5. *In vitro* HBV binding (A) and neutralization (B and C) assays of HzKR127-3.2 against *ayw* or *adr* subtypes of HBV.

Supplemental Fig. S1. Affinity determination of antibodies by competition ELISA.

Supplemental Fig. S2. Affinity determination of antibodies using Octet Red.

Supplemental Fig. S3. Crystal structure of the HzKR127 Fab–preS1 complex showing HCDR3 lid opening. The free and bound structures of HzKR127 Fab are superimposed. The CDRS of free and bound forms are shown in pink and in blue, respectively.

Supplemental Fig. S4. *In vitro* HBV neutralization assays of HzKR127-3.2 in the presence of 4% PEG against *ayw* (A) or *adr* (B) subtype of HBV.

A

```
                                FR1                        HCDR1          FR2                HCDR2
                   1       10        20        30                  40               52a       60
KR127              QVQLQQSGPELVKPGASVKISCKASGYAFS    SSWMN    WVKQRPGQGLEWIG    RIYPGDGDTNYNGKFKG
DP7                --------A-VK-------V-------T-T    -YY-H    --R-A-------M-    I-N-SG-S-S-AQ--Q-
HzKR127            --------A-V--------V----------    -----    --R-A---------    ----------AQ--Q-
HzKR127-3          --------A-VK-------V-------T-T    -----    --R-A-------M-    ----------AQ--Q-
HzKR127-3.1        --------A-VK-------V-------T-T    -----    --R-A-------M-    ----------AQ--Q-
HzKR127-3.2        --------A-VK-------V-------T-T    -----    --R-A-------M-    ---------S-AQ--Q-

                                FR3                      HCDR3        FR4
                      70          82abc      90            102        110
KR127              KATLTADKSSSTAYMQLSSLTSVDSAVYFCAR    EYDEAY   WGQGTLVTVSA
DP7                RV-M-R-T-T--V--E----R-E-T---Y---          -   ----------S
HzKR127I           ---------T-----E----R-E-T-------    ------   ----------S
HzKR127-3          RV-M-----T--V--E----R-E-T---Y---    ------   ----------S
HzKR127-3.1        RV-M-----T--V--E----R-E-T---Y---    --A---   ----------S
HzKR127-3.2        RV-M-----T--V--E----R-E-T---Y---    --A---   ----------S
```

B

```
                          FR1                    LCDR1          FR2          LCDR2
                        10        20          27abcd 30          40          50
KR127              DILMTQTPLILSVTIGQPASISC   KSSQSLLYSNGKTYLN   WLLQRPGQSPKRLIY   LVSKLDS
DPK12              --V------S----P--------   -------H-D-----Y   -Y--K---P-QL---   -V-NRF-
HzKR127            ---------S----P--------   ----------------   ----K----------   -------
HzKR127-3          --V------S----P--------   ----------------   ----K---P-Q----   ---NR--

                                FR3                      LCDR3        FR4
                     60        70        80              90          100
KR127              GVPDRFTGSGSGTDFTLKIIRVEAEDLGVYYC   VQGTHFPQT   FGGGTKLEIKR
DPK12              ------S------------S------V-----   M-SIQL-L-   ------V----
HzKR127            ------S------------S------V-----   ---------   ------V----
HzKR127-3          ------S------------S------V-----   ---------   ------V----
```

Fig. 1

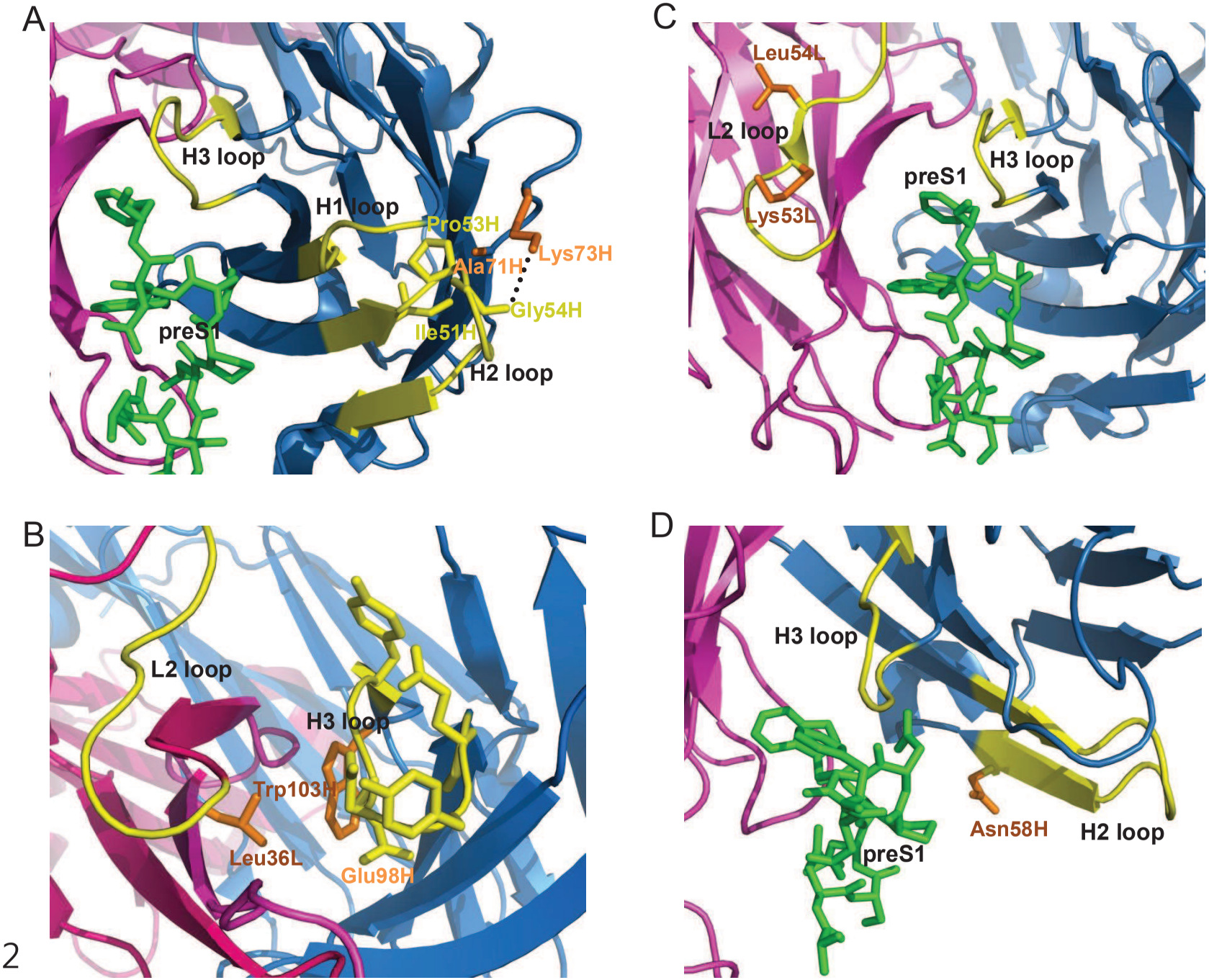
A
H3 loop
H1 loop
Pro53H
Lys73H
Ala71H
Gly54H
preS1
Ile51H
H2 loop
C
Leu54L
L2 loop
preS1
H3 loop
Lys53L
B
L2 loop
H3 loop
Trp103H
Leu36L
Glu98H
D
H3 loop
Asn58H
H2 loop
preS1

Fig. 2

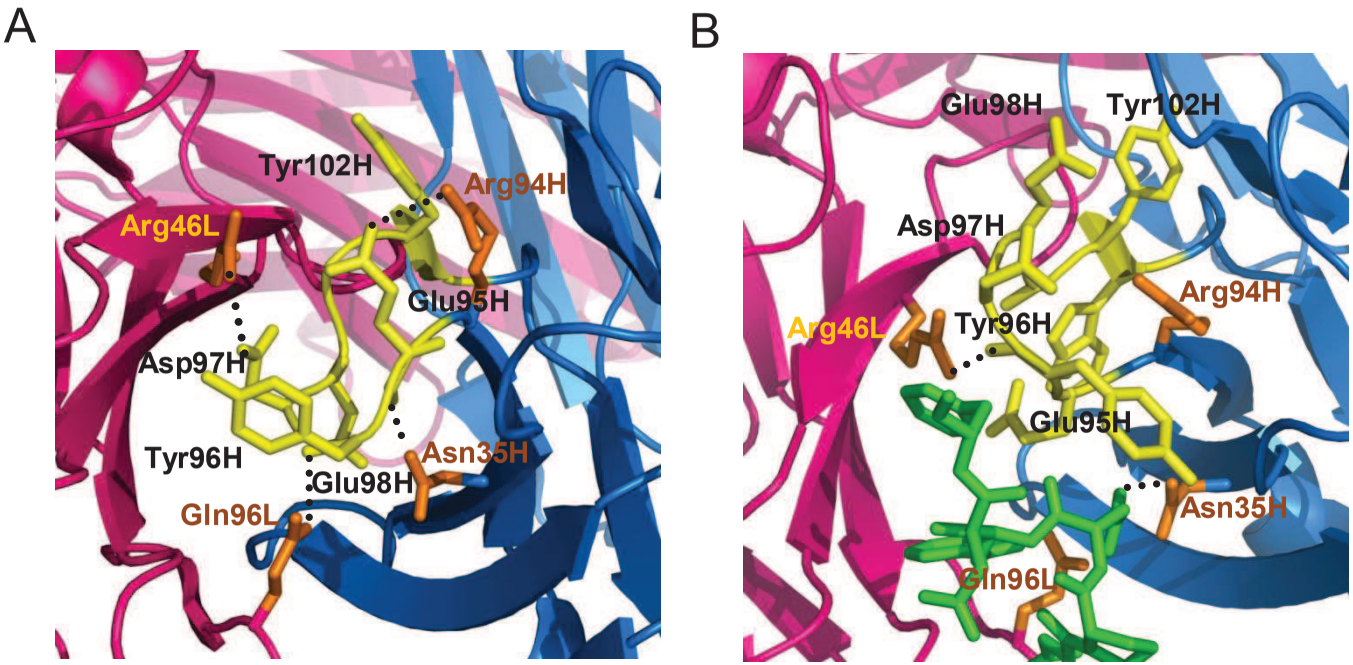
A
Tyr102H
Arg94H
Arg46L
Glu95H
Asp97H
Tyr96H
Asn35H
Glu98H
Gln96L
B
Glu98H
Tyr102H
Asp97H
Arg94H
Arg46L
Tyr96H
Glu95H
Asn35H
Gln96L

Fig. 3

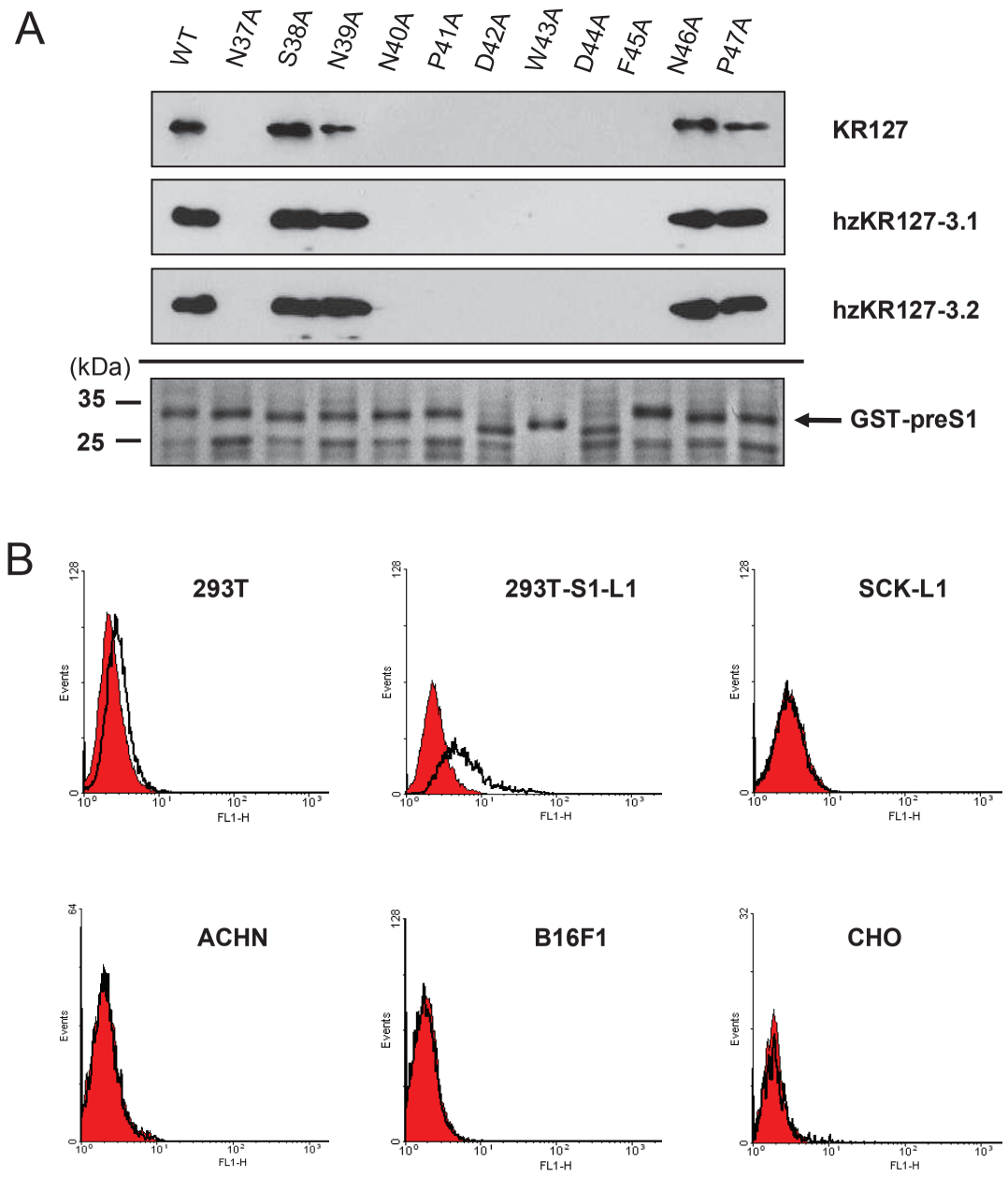
A
WT
N37A
S38A
N39A
N40A
P41A
D42A
W43A
D44A
F45A
N46A
P47A
KR127
hzKR127-3.1
hzKR127-3.2
(kDa)
35
25
GST-preS1
B
293T
293T-S1-L1
SCK-L1
ACHN
B16F1
CHO
Events
FL1-H

Fig. 4

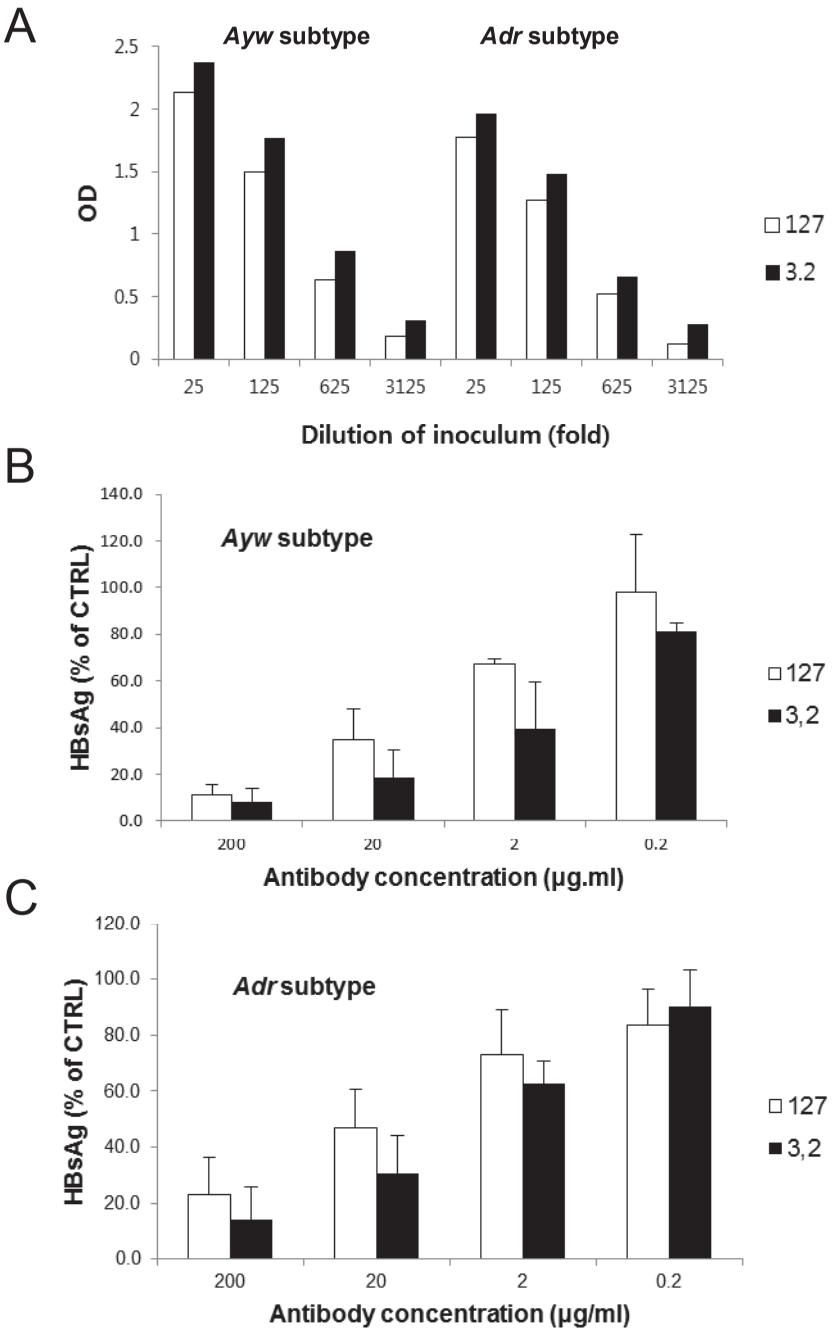
A
Ayw subtype
Adr subtype
OD
2.5
2
1.5
1
0.5
0
25
125
625
3125
25
125
625
3125
Dilution of inoculum (fold)
127
3.2
B
Ayw subtype
HBsAg (% of CTRL)
140.0
120.0
100.0
80.0
60.0
40.0
20.0
0.0
200
20
2
0.2
Antibody concentration (μg.ml)
127
3,2
C
Adr subtype
HBsAg (% of CTRL)
120.0
100.0
80.0
60.0
40.0
20.0
0.0
200
20
2
0.2
Antibody concentration (μg/ml)
127
3,2

Fig. 5

Table 1. Affinity determination of murine and humanized antibodies using Octet Red

Antibody name	K_D (M)	K_{on} (1/Ms)	K_{off} (1/s)
KR127	1.23×10^{-9}	4.68×10^{4}	5.74×10^{-5}
HzKR127-3	3.97×10^{-9}	4.23×10^{4}	1.68×10^{-4}
HzKR127-3.1	8.13×10^{-10}	5.08×10^{4}	4.13×10^{-5}
HzKR127-3.2	4.93×10^{-10}	1.08×10^{5}	5.32×10^{-5}

Table 2. Assessment of potential immunogenicity of humanized antibodies by T-cell epitope analysis. Prediction of HLA-DR binding sites by ProPred analysis (www.imtech.res.in/raghave/proped/index.html)

Antibody	**HzKR127**	**HzKR127-3.2**	**HzKR127**	**HzKR127-3.2**	**HzKR127**	**HzKR127-3.2**
Location	**HCDR2/FR3**		**FR2 in VL**		**FR2/LCDR2**	
Peptide sequence	**YNGKFKGKA**	**YAQKFQGRV**	**WLLQKPGQS**	**WLLQKPGQP**	**IYLVSKLDS**	**IYLVSNRDS**
MHC Class II molecules that Bind to peptide	DRB1_0801 DRB1_0802 DRB1_0804 DRB1_0806 DRB1_0813 DRB1_0817 DRB1_1307		DRB1_0305 DRB1_0309 DRB1_0401 DRB1_0426 DRB1_0802 DRB1_1101 DRB1_1114 DRB1_1120 DRB1_1128 DRB1_1302 DRB1_1305 DRB1_1307 DRB1_1323 DRB5_0101 DRB5_0105		DRB1_0301 DRB1_0305 DRB1_0306 DRB1_0307 DRB1_0308 DRB1_0309 DRB1_0311 DRB1_0801 DRB1_0802 DRB1_0804 DRB1_0806 DRB1_0813 DRB1_0817 DRB1_1101 DRB1_1102 DRB1_1104 DRB1_1106 DRB1_1107 DRB1_1114 DRB1_1120 DRB1_1121 DRB1_1128 DRB1_1301 DRB1_1302 DRB1_1304 DRB1_1305 DRB1_1307 DRB1_1311 DRB1_1321 DRB1_1322 DRB1_1323 DRB1_1327 DRB1_1328	DRB1_0402 DRB1_0404 DRB1_0405 DRB1_0408 DRB1_0410 DRB1_0423 DRB1_1102 DRB1_1121 DRB1_1322 DRB5_0101
Total number	7	0	15	0	33	10

Highlights

- Anti-hepatitis B virus preS1 humanized antibody was constructed by SDR grafting.
- SDR-grafted humanized antibody was affinity-matured by mutating two HCDR residues.
- Affinity matured humanized antibody exhibits enhanced HBV-neutralizing activity.
- Enhanced HBV-neutralizing activity was achieved by an increased association rate.